

Experimental Study on Focusing Multiple Atmospheric-Pressure Plasma Jets

Kiyoyuki YAMBE*, Hajime SAKAKITA, Haruhisa KOGUCHI,
Satoru KIYAMA, Nagayasu IKEDA and Yoichi HIRANO

*Energy Technology Research Institute, National Institute of Advanced Industrial Science and Technology (AIST),
Tsukuba, Ibaraki 305-8568, Japan*

(Received: 1 September 2008 / Accepted: 25 January 2009)

We have studied atmospheric-pressure plasma jets using a quartz tube and electrodes by applying low frequencies and high voltages. To increase the number of charged particles per unit area, a bundle of multiple plasma jets was concentrated at one point. To study the characteristics of the jet, the plasma was injected into a magnetic field produced by external electromagnetic coils. It was found that the plasma jet was affected by the magnetic field.

Keywords: atmospheric discharge, helium plasma jet, dielectric barrier discharge, focused multiple plasma jets, homogeneous magnetic field

1. Introduction

Recently, plasma techniques under atmospheric pressure have been adopted for industrial and biological applications. Atmospheric-pressure plasmas such as plasma jets are typically produced using an arc discharge, which produces a high-temperature plasma, whereas dielectric barrier discharge (DBD) produces a low-temperature plasma, which results in less thermal damage to a material surface [1,2].

As one of the applications of DBD, atmospheric-pressure plasma jets have been demonstrated using a quartz tube and electrodes, to which a low frequency and a high voltage were applied [3-6]. The characteristics of this type of plasma jet using helium or argon gases have been reported. A plasma plume is in fact a small bulletlike volume of plasma traveling at unusually high velocities [7-11], but a drift velocity of N_2^+ ions was estimated as almost zero [12]. The gas temperature was kept near room temperature [12,13]. The properties of the highly localized so-called "plasma bullets" that make up the plasma jet strongly resemble the properties of cathode-directed streamers in positive corona discharges [10,14,15]. It is considered that this type of plasma jet has the potential to be used as an effective plasma supplement for various types of discharge system.

In this study, we present experimental results on atmospheric-pressure discharge using a quartz tube and copper foil electrodes. A method of increasing the number of charged particles (or excited particles) per unit area is demonstrated using focused multiple plasma jets [16]. We study the dependences of the plasma jet length on the

electrode width, the distance of the electrode from the quartz tube edge, and the applied voltage. Moreover, to study the characteristics of the plasma jets, a plasma jet is injected into a homogeneous magnetic field of 0.42 T, which is externally applied using electromagnetic coils.

2. Experimental Setup

Figure 1 shows schematic diagrams of the atmospheric-pressure discharge system using a quartz tube and copper foil electrodes. As shown in Figs. 1(a) and 1(b), respectively, helium gas flows to a powered electrode (PE) from a grounded electrode (GE) (configuration A), whereas it flows to the GE from the PE in configuration B. The dielectric tube is made of quartz, and its inner diameter is $\sim\phi 1.5$ mm, thickness is ~ 0.6 mm, and length is 300 mm. The PE and GE are made of copper foil with a thickness of 0.2 mm. In the figure, L indicates the distance between the downstream electrode and the quartz tube edge. Here, the plasma jets on the PE and GE sides are defined as PEJ and GEJ, respectively.

We use two types of power supply system. The first type is referred to as PSA (LHV-13A, Logy Electric Co.) and has a maximum voltage of $\sim\pm 10$ kV and a frequency of ~ 10 kHz (see Fig. 2(a)). In the case of PSA, the distance between the electrodes is set at 6 mm. PSA is used to study the plasma jet length dependences on electrode width and electrode configuration. The second type is referred to as PSB (PHF-2KH, Hiden Laboratory Co.) and has a maximum voltage of ± 15 kV and a frequency range of 1 to 100 kHz (see Fig. 2(b)). In the case of PSB, the distance between the electrodes is set at

*Present affiliation: Osaka University

Author's e-mail: k-yambe@ppl.eng.osaka-u.ac.jp

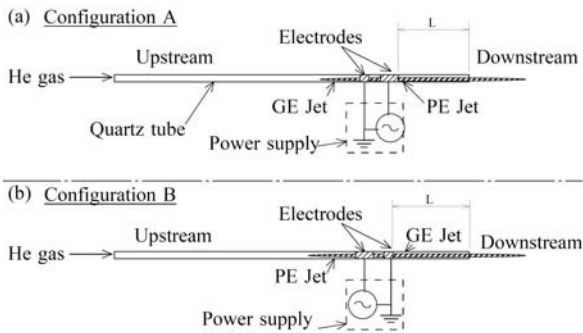


Fig. 1. Schematic drawings of atmospheric-pressure discharge system using quartz tube and electrodes.

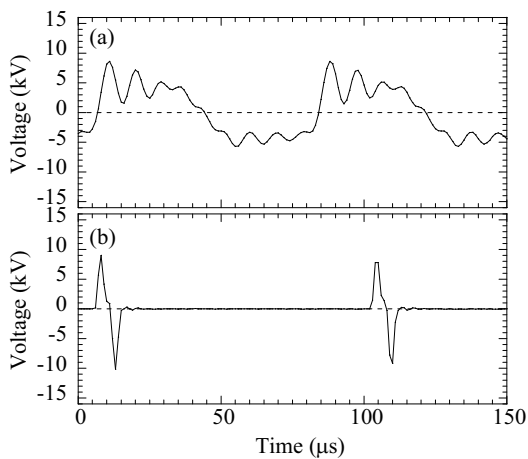


Fig. 2. Time evolutions of applied voltage on powered electrode for power supplies (a) PSA and (b) PSB.

15 mm. PSB is used to study the plasma jet length dependences on the voltage and frequency of pulses. It is possible to produce a plasma jet using not only bipolar pulses but also unipolar pulses (both positive and negative), although the results will be described in detail in future reports. The plasma jet length is measured using CCD camera images.

3. Experimental Results

3.1 Focused multiple plasma jets

We demonstrate a method of increasing the number of charged particles per unit area using focused multiple plasma jets. Figure 3 shows an example of focused atmospheric-pressure plasma jets. Basically, the same discharge principle is adopted as that shown in Fig. 1. Five sets of plasma jets are focused at the focal point (three tubes are shown, and the other two are located behind). Here $PE_w = 10$ mm, $GE_w = 5$ mm, $L = 27$ mm, and the PSA power supply is used for configuration B. PE_w and GE_w are defined as the widths of PE and GE, respectively. In Fig. 4(a), five plasma jets are focused at the focal point. It is difficult to identify the focal point owing to the limitation of the gradation level of the CCD camera; however, it is confirmed by the naked eye that the five

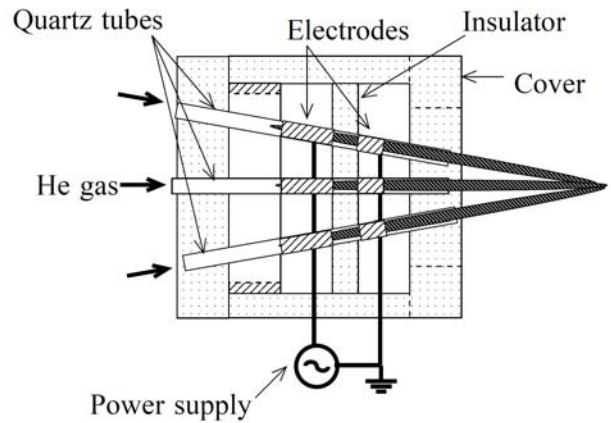


Fig. 3. Example of focused atmospheric-pressure plasma jets.

plasma jets are focused at one point. In the case of two sets of plasma jets, the mixing point of each jet can be clearly identified as shown in Fig. 4(b). A future problem is to confirm the number of charge particles around the focal region. The gas flow rate is an important parameter in controlling the jet focusing. In the case of Fig. 4(b), the gas flow rate is ~ 8.0 l/min, which is rather large, but the jet does not exhibit turbulent behavior.

3.2 Dependence of plasma jet length on electrode configuration

A plasma plume forms a small bulletlike volume of plasma traveling in a narrow quartz tube with an inner diameter $\phi 2$ mm [10]. To study a shape of the plasma in a large diameter tube, a quartz tube of diameter $\phi 15$ mm and thickness 1.5 mm is used. In this case, the plasma is produced in the form of concentric circles around the inner surface of the quartz tube as shown in Fig. 5(a). The plasma jet is very short on the downstream side, however, on the upstream side, the plasma jet is relatively long and forms a narrow jet that tapers off away from the electrode as shown in Fig. 5(b).

The plasma jet length (L_j) dependences on PE_w and GE_w are shown in Fig. 6. Here $L = 97$ mm and PSA is used for configuration A. The lengths of PEJ and GEJ are denoted by L_j^P (downstream side) and L_j^G (upstream side), respectively. Both L_j^P and L_j^G increase with PE_w ; however,

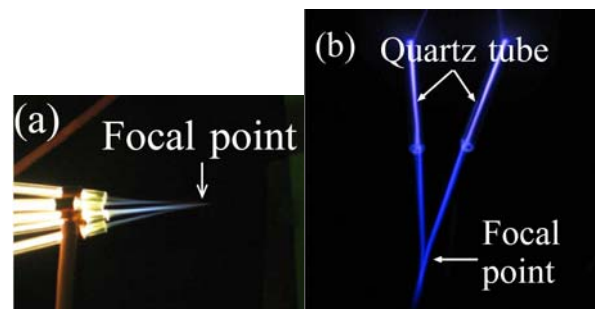


Fig. 4. Photographs of focused multiple plasma jets: (a) five sets of jets and (b) two sets of jets.

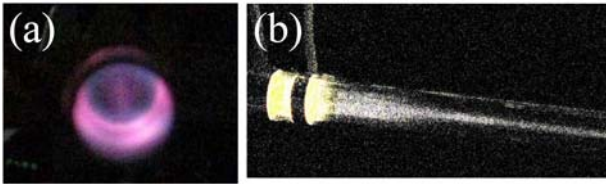


Fig. 5. Photographs of quartz tube of diameter $\phi 15$ mm and thickness 1.5 mm: (a) front view and (b) side view (color contrast has been adjusted).

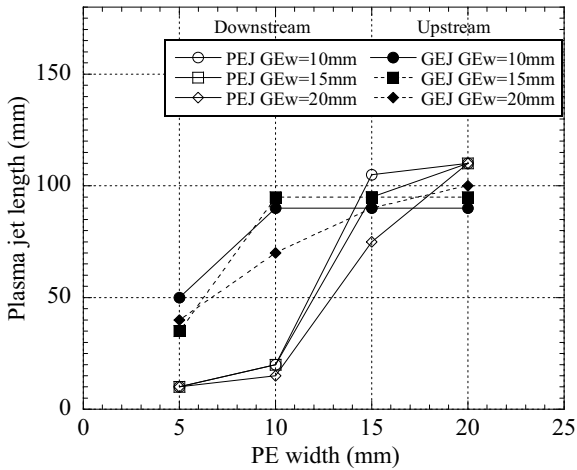


Fig. 6. Dependences of plasma jet length on the widths of PE and GE in configuration A.

there is no clear dependence on GE_w .

Figure 7 shows the dependences of L_j on PE_w and GE_w for $L = 97$ mm when PSA is used for configuration B. Both L_j^P (upstream side) and L_j^G (downstream side) increase with PE_w ; however, they do not depend on GE_w .

3.3 Dependence of plasma jet length on distance of electrode from quartz tube edge

The dependences of L_j^P and L_j^G on the distance of the electrode from the quartz tube edge, L , are shown in Fig. 8.

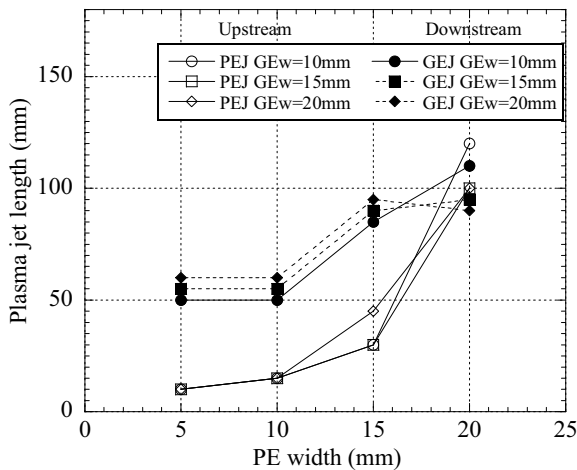


Fig. 7. Dependences of plasma jet length on the widths of PE and GE in configuration B.

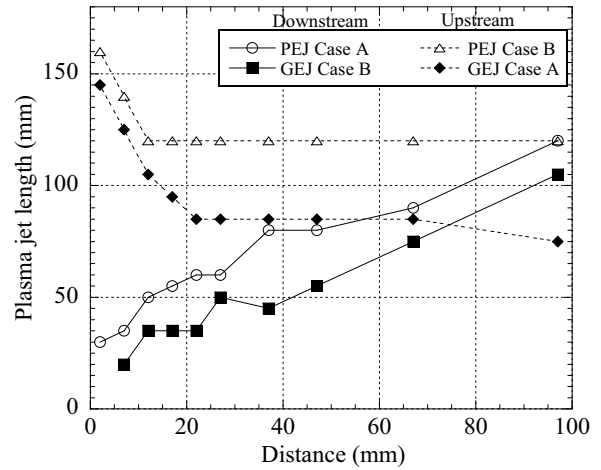


Fig. 8. Dependences of plasma jet length on distances of electrode from quartz tube edge.

Here $PE_w = 20$ mm, $GE_w = 5$ mm, and PSA is used. The plasma jet lengths on the downstream and upstream sides show a similar trend with changing L . In both configurations A and B, L_j on the upstream side is longer than that on the downstream side, particularly when $L < 30$ mm, and L_j^G becomes constant when $L > 30$ mm. On the other hand, L_j on the downstream side increases in proportion to L . The plasma jet becomes long at the powered electrode side. L_j^P is about $L + 23$ mm.

3.4 Dependences of plasma jet length on applied voltage and frequency

The dependences of L_j^P and L_j^G on the applied voltage and frequency using PSB are shown in Fig. 9 for configuration A with $PE_w = 20$ mm, $GE_w = 5$ mm, and $L = 27$ mm. Each plasma jet length increases in proportion to voltage; however, the jet length does not depend on frequency for frequencies between 5 and 20 kHz. Plasma jet production in a high frequency region of 100 kHz was reported in ref. 8.

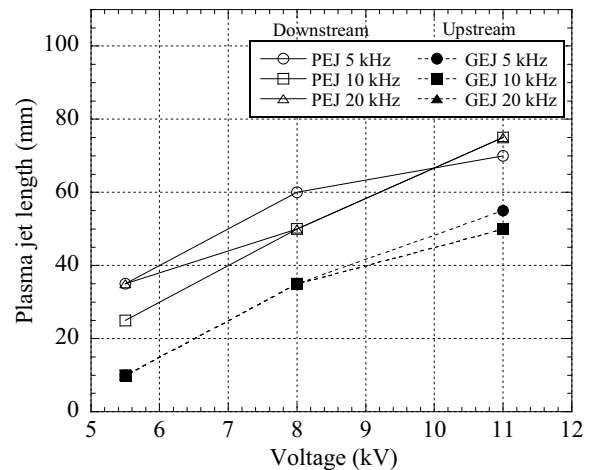


Fig. 9. Dependences of plasma jet length on voltage and frequency.

3.5 Interaction with the magnetic field

To study the characteristics of the plasma jets, a plasma jet is vertically injected into a homogeneous magnetic field of $B = 0.42$ T, which is generated using electromagnetic coils. Figure 10 shows a photograph of the electromagnetic coils, discharge system, and image measurement system. Here $PE_w = 20$ mm, $GE_w = 5$ mm, $L = 27$ mm, and PSA is used with configuration A. The plasma jets shown in Fig. 11 were obtained under the following conditions: (a) without plasma, (b) plasma without a magnetic field, (c) plasma with a magnetic field in the direction from right to left and (d) plasma with a magnetic field applied from left to right. The plasma jet flows from right to left without a magnetic field, as shown in Fig. 11(b). However, in Fig. 11(c) it can be seen that the upper part of the plasma jet is suppressed or disappears. In Fig. 11(d), where the direction of the magnetic field is opposite that in the Fig. 11(c), the downward part of the plasma jet is suppressed or disappears. As results, it was found that the plasma jet was affected by the homogeneous magnetic field. The mean free path of ions and electrons with neutral particles is very short under atmospheric-pressure. Therefore, it is difficult to explain the interaction mechanism in terms of the Lorentz force.

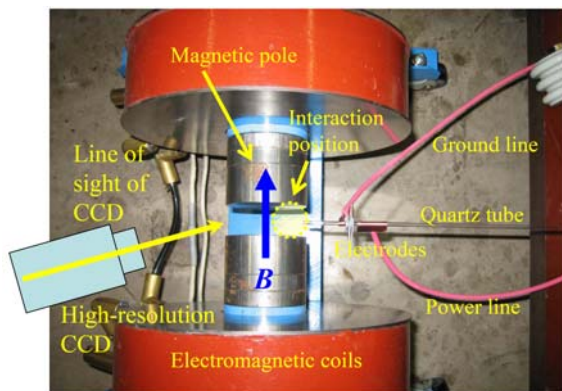


Fig. 10. Photograph of electromagnetic coils, discharge system, and image measurement system.

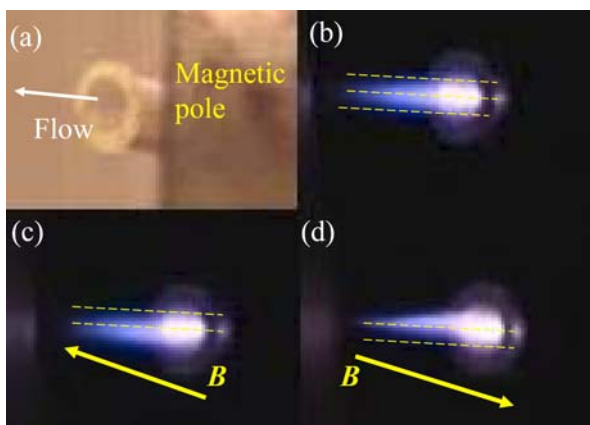


Fig. 11. Photographs of plasma jets: (a) without plasma, (b) without magnetic field B , (c) with B , and (d) with B (opposite direction to that in (c)).

We must further study the origin of the above phenomena from several viewpoints.

4. Summary

We demonstrated a method of increasing the number of charged particles (or excited particles) per unit area using focused multiple plasma jets under atmospheric-pressure conditions. Multiple sets of plasma jets were successfully focused at one point, although the relation between the density (or emission intensity) and the number of jets is yet to be studied. Moreover, we studied the characteristics of atmospheric-pressure plasma jets using a quartz tube and copper foil electrodes, to which low frequencies (~ 10 kHz) and high voltages (~ 10 kV) were applied. The plasma jet length increased as the width of the powered electrode increased and the applied voltage increased. When the plasma jet was injected into a homogeneous magnetic field, it was found that the plasma jet was affected. This cause of this phenomenon is an open question at present.

Acknowledgments

Part of this study was financially supported by the Budget for Nuclear Research of the Ministry of Education, Culture, Sports, Science and Technology of Japan, based on the screening and counseling of the Atomic Energy Commission. We thank Takano Giken Inc. for their support by providing the electromagnetic coil.

References

- [1] S. Kanazawa *et al.*, J. Phys. D: Appl. Phys. **21**, 838 (1988).
- [2] S. Okazaki *et al.*, J. Phys. D: Appl. Phys. **26**, 889 (1993).
- [3] M. Teschke *et al.*, IEEE Trans. Plasma Sci. **33**, 310 (2005).
- [4] M. Teschke *et al.*, Proc. 48th Annual Tech. Conf. Soc. Vac. Coasters 505/856-7188, 1 (2005).
- [5] K. Tachibana, 5th AIST Forum on Mezzo-technology, Tsukuba (2006) [unpublished].
- [6] J. L. Walsh and M. G. Kong, IEEE Trans. Plasma Sci. **36**, 954 (2008).
- [7] X. P. Lu and M. Laroussi, J. Appl. Phys. **100**, 063302 (2006).
- [8] H. Motomura *et al.*, Jpn. J. Appl. Phys. **46**, L939 (2007).
- [9] J. Shi *et al.*, Phys. Plasmas **15**, 013504 (2008).
- [10] B. L. Sands *et al.*, IEEE Trans. Plasma Sci. **36**, 956 (2008).
- [11] R. Ye and W. Zheng, Appl. Phys. Lett. **93**, 071502 (2008).
- [12] K. Urabe *et al.*, Appl. Phys. Express **1**, 066004 (2008).
- [13] J. L. Walsh and M. G. Kong, Appl. Phys. Lett. **91**, 221502 (2007).
- [14] K. Kitano and S. Hamaguchi, Proc. 18th Int. Symp. Plasma Chem. 211 (2007).
- [15] B. L. Sands *et al.*, Appl. Phys. Lett. **92**, 151503 (2008).
- [16] H. Sakakita *et al.*, Proc. 25th Symp. Plasma Processing 137 (2008).